ELSEVIER

Chemical Engineering Journal 138 (2008) 239–248

Chemical Engineering Journal

www.elsevier.com/locate/cej

Kinetics and equilibrium studies of the herbicide 2,4-dichlorophenoxyacetic acid adsorption on bituminous shale

Nihat Ayar, Binay Bilgin, Gülten Atun *

Istanbul University, Department of Chemistry, Faculty of Engineering, 34320 Avcılar-Istanbul, Turkey

Received 8 April 2007; received in revised form 21 June 2007; accepted 29 June 2007

Abstract

The adsorptive removal of the herbicide 2,4-dichlorophenoxyacetic acid (2,4-D) by bituminous shale (BS) has been studied by means of batch technique. Kinetic data well fit to McKay equation at the lowest initial concentration of 6×10^{-5} M, which assumes a two-resistance diffusion model. The effective film-diffusion coefficients, which correspond to initial fast stage of the adsorption, are in the magnitude $\sim 10^{-11}$ m^2/s whereas particle-diffusion coefficients corresponding to the latter slow stage are $\sim 10^{-14}$ m^2/s in the studied concentration range of $(0.6–4.0) \times 10^{-4}$ M. Both film- and particle-diffusion coefficients decrease as the initial concentration increases while the effective diffusion coefficient of 7.73×10^{-13} m^2/s calculated from Paterson's equation based on a one-resistance diffusion model changes neither initial concentration nor temperature. Average activation energies calculated by applying Arrhenius equation to film-diffusion coefficients are found to be positive whereas they change around zero for particle-diffusion process. Thermodynamic parameters estimated according to Eyring equation based on the transition state theory indicate the existence of both energy and entropy barrier in the system.

Experimental equilibrium data points are found in accordance with the curves calculated according to Freundlich, Dubinin–Radushkevich (D–R) and Langmuir isotherm equations. Adsorption capacities of the BS for 2,4-D calculated from isotherm parameters increase with increasing temperature and decreasing pH.

Keywords: 2,4-D; Bituminous shale; Adsorption kinetics; McKay equation; Paterson's equation; Adsorption equilibrium

1. Introduction

Pesticides are major pollutants of both surface- and groundwater because of their usage in open environment. Adsorption is one of the most promising techniques for pesticide removal due to flexibility in design and operation. Batch and/or column experiments have been undertaken to study adsorption characteristics of some pesticides such as (2,4-dichlorophenoxy) propanoic acid (dichlorprop), (4-chloro-2-methylphenoxy) propanoic acid (mecoprop) [1], (4-chloro-2-methylphenoxy) acetic acid (MCPA) [1–4], picloram [4], 2,4-dichlorophenol (DCP), 2-methyl-4-chlorophenol (MCP) [1,5] dimethoate [6], clofencet [7], benazolin [8], atrazine [9], carbofuran [10], 2,4-D [1,4–15], Deltamethrin and Lambda-Cyhalothrin [16]. The choosing of a suitable adsorbent for pesticide removal is a complex problem because of the wide variety of their chemical structures. Although adsorption on activated carbon is the most widespread technology dealing with purification of water contaminated by pesticides [8,11] due to its high cost some cheaper and commercially available materials such as clay minerals [2,14], hydrous oxides [3,4,12,13,15], industrial by products [9,10], bituminous shale [5] and oil shale ash [16] have been used for pesticide removal.

Chlorinated phenolic organic compounds are an important class of the pesticides. 2,4-D is a widely used anionic pesticide in agriculture leads to increase amount of this compound in food and drinking water. The resulting 2,4-DCP from 2,4-D may lead to an additional risk for environmental pollution. Since anionic pesticides are very weakly retained by most of the soil components because of their structural negative charge they remain dissolved in the soil solution and can rapidly move around leading subsequent contamination of surface and ground waters. Although some of studies on 2,4-D adsorption are focused on its partition in soil components [1–6,7] they are also considered as a water treatment method for the removal purposes [4,5,8–12].

* Corresponding author. Tel.: +90 4737031; fax: +90 4737180.
E-mail address: gultena@istanbul.edu.tr (G. Atun).

1385-8947/$ – see front matter © 2007 Elsevier B.V. All rights reserved.
doi:10.1016/j.cej.2007.06.032

2,4-D is a member of phenoxyalkanoic acid herbicides having one polar carboxylic group and one lipophilic phenyl moiety. Its carboxylic group can interact both with organic matter surfaces groups in soils and also negatively charged clays via metal ion bridges as well as it can be partitioned in organic matters by means of lipophilic interactions [1,17–19]. Therefore, both carbonaceous and siliceous materials have been used as adsorbent for the removal of 2,4-D from contaminated aqueous solutions. Using activated carbon as a reference [8,11] investigations are focused on some inexpensive materials and their activated forms such as silica gel activated with 3-(trimethoxysilyl)-propylamine [12,13], tire rubber granules [9], organophilic sepiolite [14], calcined anionic clay Mg–Al–CO_3–LDH [4], layered double hydroxides [15], fertilizer industry waste (carbon slurry) and steel industry wastes (blast furnace slag, dust, and sludge) [10].

Adsorption is an economical treatment process for the removal of water pollutants especially using locally available low cost adsorbents. Bituminous shale is an argillaceous oil shale that contains bitumen, a mixture of hydrocarbons that may be used as fuel [20,21]. Although the oil shales are potentially an important alternative energy source for oil supplement the deposit located in Göynük near Bolu in Turkey is considered to be uneconomic on the basis of oil yield. Göynük deposit with reserves estimated 10^9 t is the largest in Turkey having 5 billion tons of oil shale in seven areas of western and central Anatolia [22–24]. Currently, researches are directed toward development of alternate uses for oil shale such as the preparation of clean solid fuel, admixture in building industry and adsorbent for waste management [5,20,21,25–27]. Oil shales are sedimentary rocks composed of tightly bounded inorganic and organic materials. The inorganic matter in oil shale consists of some clay minerals such as montmorillonite, feldspar, quartz and dolomite. Kerogens in organic matter are insoluble in organic solvents because of their three-dimensionally crosslinked polymer structure [22,26,28,29]. The macromolecular network properties of kerogens in the BS and carbonates, silicates and sulfates in its ash suggest that it might be have a potential for pesticide adsorption [5,16]. The aim of this study is to determine adsorption characteristics of BS for 2,4-D removal.

2. Experimental

2.1. Adsorbate specifications

The herbicide 2,4-D was supplied from Atabay Pharmaceutical Products Inc. (Turkey) and used without purification. Its melting point, solubility in water at 298 K and pK_a value are 413.5 K [6], 620 mg/l [6] and 2.6 [7], respectively.

2.2. Preparation and specifications of the adsorbent

Physical and chemical characteristics of oil shale are estimated by measuring the total volatile and organic matters, moisture and ash content, and total sulfur and carbonates [30]. The reported chemical and mineralogical analysis of the shale which provided from Göynük region (in Bolu, Turkey) are as follows [5,29]: moisture, 5.7%; ash, 24.4%; volatile matter, 56.3%; and fixed carbon, 13.6%; C, 49.92%; H, 6.42; S, 3.32%; N, 1.07%; and O, 9.4%. The raw shale contained 8.1% bitumen and its ash consisted of 52.5% (carbonate + sulfate), 23.1% silicate, 1.1% pyrite, 1.1% bitumen and 21.4% kerogen which is a bitumen like solid composed of a mixture of aliphatic and aromatic compounds. Inorganic materials accompanying kerogen are matrix-bound and consisted of plagioclase mineral.

In order to remove impurities and soluble components in acid media following acid activation procedure was applied to the adsorbent as reported in literature [5]. One hundred grams of bituminous shale were treated with HCl solution of 15% (w/w) at 353 K for 2 h in a thermostatic shaker. After decantation and removal of the aqueous acid solution, the solid was separated and washed with water up to pH 5.5–6.0, dried at 403 K. The BS crushed and sieved through 250–500 μm sieves to be used for adsorption experiments.

Chemical analysis of the BS after acid treatment is as follows: moisture, 1.3%; ash, 21.2%; volatile matter, 57.5%; and fixed carbon, 20.0%; C, 62.20%; H, 8.68; S, 1.72%; N, 1.55%; and O, 12.5%.

It can be seen from XRD patterns in Fig. 1, the BS consists of plagioclase type feldspar, pyrite and gypsum. It can be concluded that from the comparison of XRD patterns of the raw and acid treated BS the matrix bound inorganic minerals are not soluble in dilute acid and acid treatment does not cause a significant change in the matrix composition [5,29].

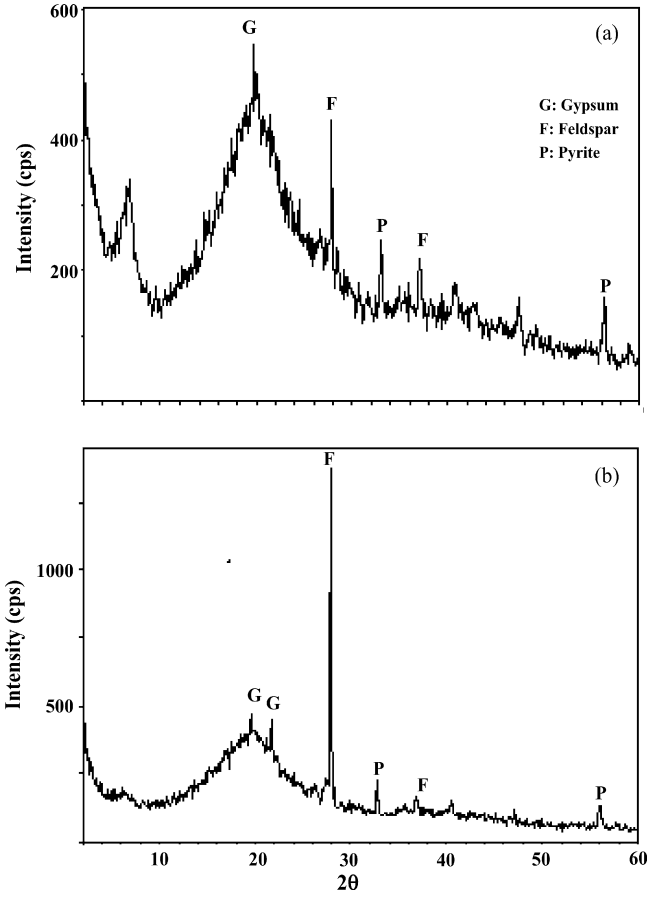

Fig. 1. XRD patterns: (a) the raw and (b) the acid treated BS.

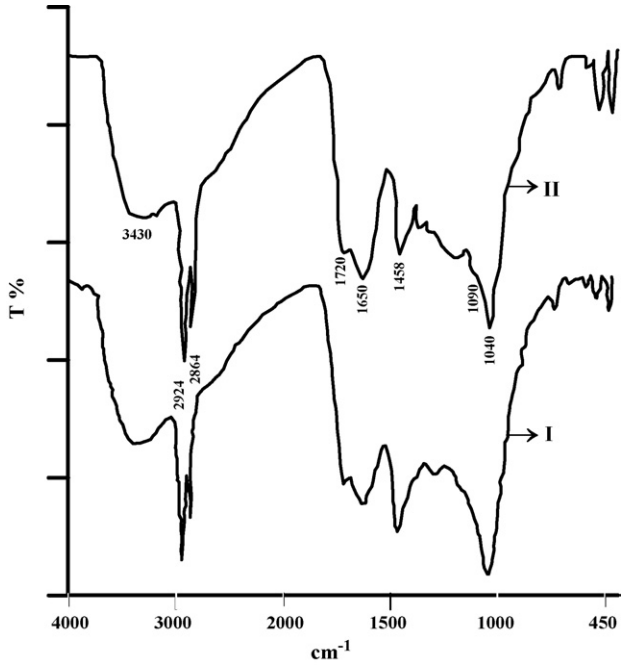

Fig. 2. A comparison of FTIR spectra of the raw (I)—and the acid treated BS (II).

FTIR spectra of the raw and acid treated BS are compared in Fig. 2. They give useful information about structures especially for determination of types and intensities of surface functional groups such as hydroxyl and carboxyl groups. No significant change is observed in surface functional groups after acid treatment. Two strong bands observed at 2924 and 2864 cm^{-1} are assigned to asymmetric C–H and symmetric C–H bands, respectively, presented in alkyl groups such as methyl and methylene groups. The broad band located at 3430 cm^{-1} is attributed to hydrogen bonds participating in adsorbed water molecules. The band at 1650 cm^{-1} is due to O–H bonding. The bands between 1400 and 1800 cm^{-1} may be attributed to presence of coupled carbonyl groups and systems of aromatic rings stretching. The band at 1458 cm^{-1} is attributed to $–CH_2$ rocking. The shoulder at 1720 cm^{-1} ascribed to stretching vibration of carbonyl groups on the edges of the layer planes and/or to the double bonds in carboxylic acid and lactone groups. The absorption band at 1040 cm^{-1} as well as the shoulder at 1090 cm^{-1} is assigned to Si–O bonding [31,32]. Chemical, mineralogical and structure analysis of the adsorbent were carried out using Thermo Finnigan Flash EA 1112 Series element analyzer, Rigaku D/Max-2200/PC XRD and Perkin-Elmer Precisely Spectrum One FTIR instruments.

Surface site concentration arising from hydroxyl and carboxyl groups was determined as 2.06×10^{-4} mol/g using acid–base titration method. Surface area of the adsorbent determined by nitrogen gas adsorption BET method was 11.0 m^2/g. The particle density was determined as 1.44 g/cm^3 by using a Wertheim pycnometer of 10 cm^3 capacity coupled with a thermometer. The estimated uncertainty of the measured density is ±0.01 g/cm^3 at 298 K.

2.3. Adsorption experiments

Adsorption experiments were carried out by means of the batch method using 2,4-D solutions in the concentration range of (0.6–4.0) $\times 10^{-4}$ M at the temperatures of 298, 308, 318 and 328 K. In order to obtain relevant data for kinetic calculations a fixed amount of the adsorbent (0.2 g) was shaken with 10 cm^3 of the solution at a given concentration for 15, 30, 60, 120, 180, 240 and 300 min at constant temperatures in a thermostatic shaker/water bath. The equilibrium studies were performed for 24 h. After centrifugation at 4000 rpm for 10 min concentration of 2,4-D was measured with a Unicam UV2-100 UV–vis spectrophotometer at 282 nm. All of the batch tests were performed in glass bottles in duplicate and average values were used in the calculation. Deviations are less than 2%.

Natural pH of 2,4-D solutions is around 5.6. In order to study the effect of pH on 2,4-D adsorption initial pHs of the solutions were adjusted from 3.5 to 8.0 by adding 0.1 M HCl or 0.1 M NaOH. Ionic strength of the solutions was kept constant at 10^{-3} M by adding required amount of NaCl. Uncertainty in the pH values in the concentration range studied was ±0.1.

3. Results and discussion

3.1. Application of kinetic models

The time dependent adsorbed fraction F_t was determined for whole concentration range studied as follows and represented in Fig. 3a for initial concentration of 6.0×10^{-5} M at different temperatures:

$$F_t = \frac{C_0 - C_t}{C_0} \tag{1}$$

$$F_t = \frac{\bar{C}_t}{C_0} \tag{2}$$

where C_0 and C_t are adsorbate concentrations in the aqueous phase at initial and time t, so $\bar{C}_t$ is the concentration in solid phase (in mol/l).

As shown in Fig. 3a, a slower process follows a rapid initial uptake. McKay and Paterson's equations could be applied to the kinetic data based on two- and one-resistance diffusion models, respectively [33,34].

McKay equation, which assumes film- and particle-diffusion, can be written as follows [21]:

$$\ln(1 - F_t) = -k(C_t + \bar{C}_t)t \tag{3}$$

In order to analyze the $\ln(1 - F_t) = f(t)$ curves in Fig. 3b plotted according to McKay equation the final linear portion is extrapolated back to $t = 0$. A straight line represented in the inset in Fig. 3b, whose slope is correlated to the rate constant of initial fast process (k_1, in l/mol s), is obtained subtracting the extrapolated line from the original curve. The film-diffusion coefficient D_f (in m^2/s) can be calculated from the following relation by

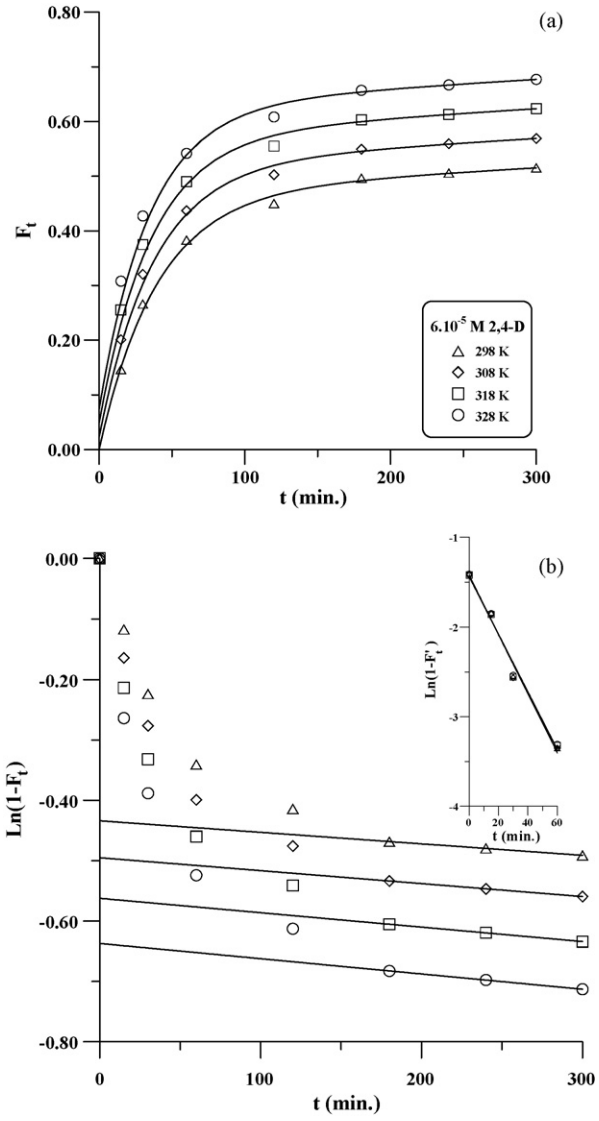

Fig. 3. (a) Time dependencies of adsorbed fractions in 6.0×10^{-5} M 2,4-D solutions at different temperatures, (b) McKay plots for calculation k_2 as well as D_f, the inset: McKay plots for calculation k_1 as well as D_p (the curves in (a) have been calculated using the McKay constants derived from (b)).

using the k_1 values [35,36]:

$$D_f = k_1 \frac{V\delta\bar{C}_\infty}{A} \tag{4}$$

where V is the solution volume, δ the thickness of liquid film, A the specific surface area of the adsorbent and $\bar{C}_\infty$ the adsorbate concentration in solid phase determined from the intercept of extrapolated line.

The rate constant k_2 (in l/mol s) corresponding to the slow process is determined from the slope of extrapolated straight lines in Fig. 3b according to following equation:

$$\ln(1 - F_t) = A - k_2(C_t + \bar{C}_t)t \tag{5}$$

When the particle-diffusion contributes on adsorption process by assuming that the diffusion is radial direction following equation can be used to obtain adsorbed fraction [35,36]:

$$F_t = 1 - \sum_{n=1}^{\infty} \frac{6\alpha(\alpha+1)}{9 + 9\alpha + \alpha^2 q_n^2} e^{-D_p q_n^2 t / r_0^2} \tag{6}$$

Thus,

$$\ln(1 - F_t) = A - \frac{D_p q_1^2}{r_0^2} t \tag{7}$$

where $A = \ln[6\alpha(\alpha+1)]/(9 + 9\alpha + \alpha^2 q_1^2)$, r_0 the mean radius of particles, q_n's are the non-zero roots of $\tan q_n = (3q_n)/(3 + \alpha q_n^2)$ and $\alpha = (3V)/(4\pi r_0^3)$ represents the volume ratio of external solution to the solid particles. Constant k_2 can be correlated to D_p with a combination of Eqs. (5) and (7) as follows:

$$D_p = k_2 \frac{(C_t + \bar{C}_t) r_0^2}{q_1^2} \tag{8}$$

The calculated values of k_1 and k_2 depending on initial concentration were presented in Fig. 4 and in its inset, respectively. Using the of k_1 and k_2 values calculated F_t versus t curves according to McKay model are compared to experimental points in Fig. 3a. As it is seen in Fig. 3a experimental data well predicted by McKay model in the lowest concentration of 2,4-D solution at four temperatures.

Amounts of solute adsorbed (q_t in mol/g) up to equilibrium are plotted against contact time at five initial concentrations depending on temperature in Fig. 5(a–e). As easily can be seen from Fig. 5(a–e), although modeled curves according to McKay equation (dashed curves) are well consistent with experimental points at the lowest concentration they deviate as initial concentration increases. Standard deviations between experimental and calculated q_t values are also shown in the Fig. 5(a–e).

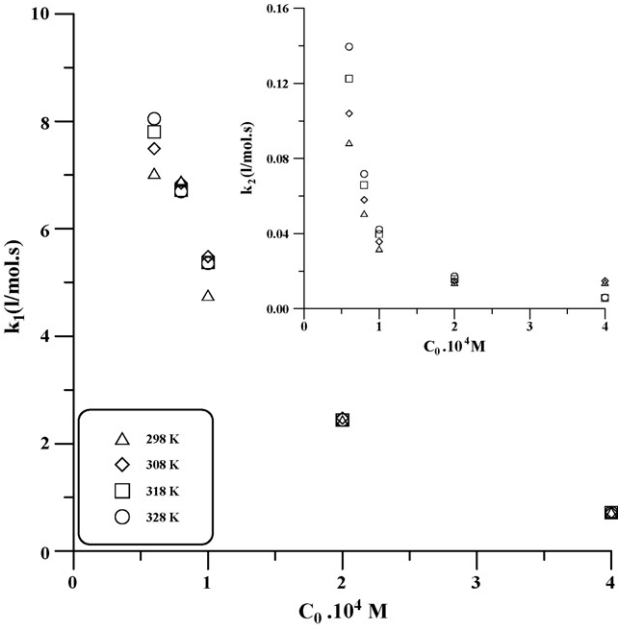

Fig. 4. The changes of McKay constants depending on initial concentration of 2,4-D solutions.

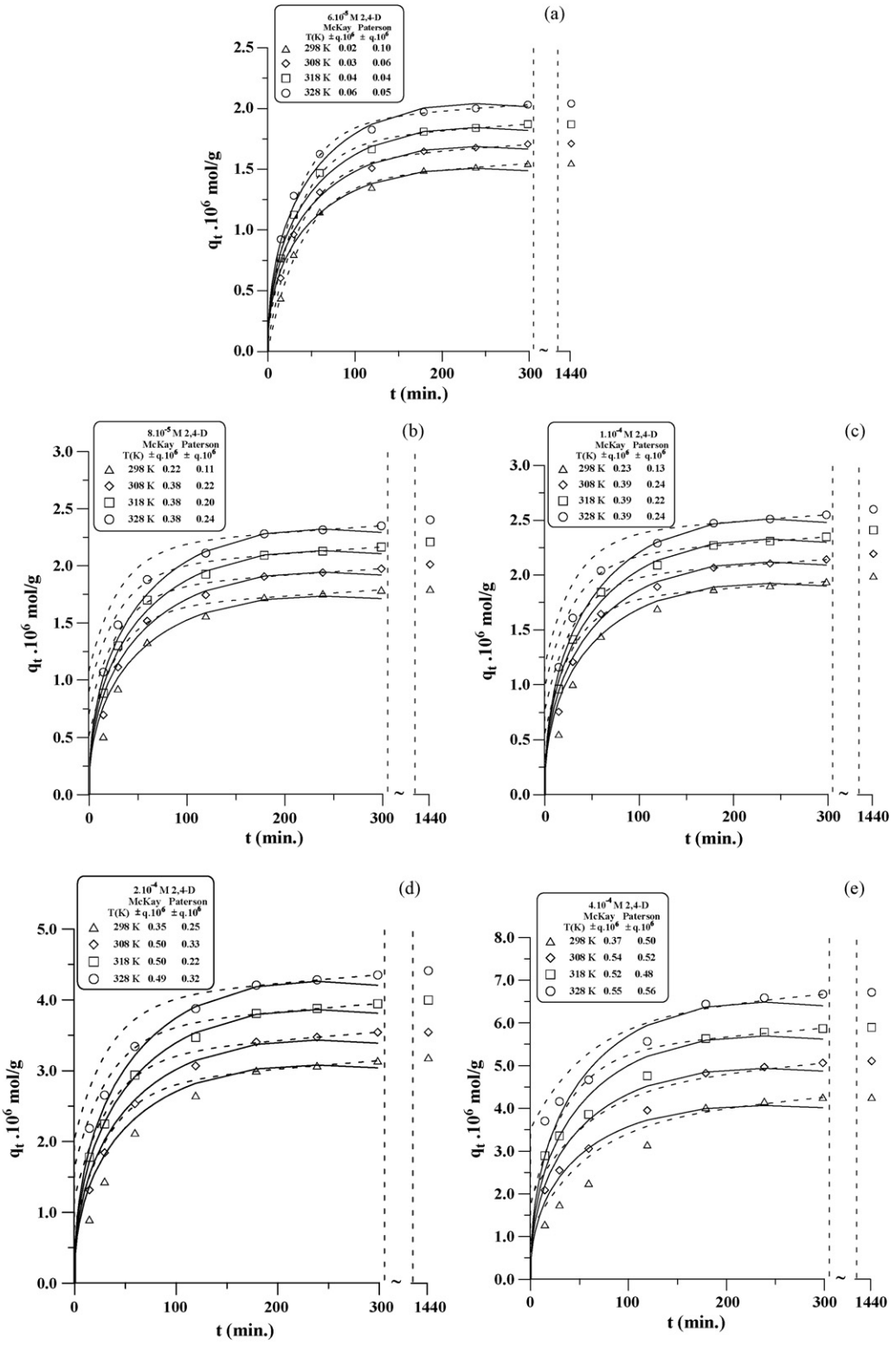

Fig. 5. Amounts of solute adsorbed at different temperatures in 2,4-D solutions of: (a) 6.0×10^{-5} M, (b) 8.0×10^{-5} M, (c) 1.0×10^{-4} M, (d) 2.0×10^{-4} M and (e) 4.0×10^{-4} M. (Solid and dashed curves have been calculated using Paterson and the McKay constants, respectively.)

Paterson's equation, which assumes a constant particle-diffusion coefficient independent of initial solution concentration, was also applied to the data [34]. Typical adsorption kinetics is described in terms of fractional attainment of equilibrium U_t at time t and determined experimentally as follows:

$$U_t = \frac{q_t}{q_e} \tag{9}$$

Table 1
Effective diffusion coefficients and activation parameters for 2,4-D adsorption on the BS

Model	$C_0 \times 10^4$ (M)	D_0 (m^2/s)	ΔE_a* (kJ/mol)	ΔH* (kJ/mol)	ΔG* (kJ/mol)	ΔS* (kJ/mol K)	r
H. McKay (1st)	0.6	1.76×10^{-11}	11.51	8.92	39.64	−0.10	0.999
	0.8	0.32×10^{-11}	7.02	4.42	39.33	−0.12	0.999
	1.0	1.10×10^{-11}	10.67	8.07	39.94	−0.11	0.964
	2.0	0.59×10^{-11}	9.75	7.15	40.54	−0.11	0.997
	4.0	1.19×10^{-11}	13.81	11.22	42.89	−0.11	0.999
H. McKay (2nd)	0.6	5.26×10^{-14}	2.85	0.25	45.36	−0.15	0.918
	0.8	3.72×10^{-14}	2.39	−0.21	45.75	−0.15	0.888
	1.0	0.72×10^{-14}	−1.36	−3.96	46.06	−0.17	0.962
	2.0	1.54×10^{-14}	0.69	−1.91	46.24	−0.16	0.821
	4.0	0.19×10^{-14}	−4.24	−6.84	46.55	−0.18	0.805
Paterson	0.6–4.0	7.73×10^{-13}	0.00	−2.60	35.86	−0.13	1.000

In order to determine U_t according to Paterson's model the following equation was employed [34,37]:

$$U_t = \frac{w+1}{w}\{1 - f_1[f_2(1+f_3) - f_4(1+f_5)]\} \quad (10)$$

here, $f_1 = 1/(a-b)$, $f_2 = a\exp(a^2P)$, $f_3 = \mathrm{erf}(aP^{1/2})$, $f_4 = b\exp(b^2P)$, $f_5 = \mathrm{erf}(bP^{1/2})$; a and b roots of equation: $x^2 + 3wx - 3w = 0$ $(a > b)$, $w = \bar{C}_e\bar{V}/C_eV$, $\bar{C}_e$ and C_e are equilibrium concentrations in solid and solution phases and $\bar{V}$ is the volume of the solid phase, and $P = D_pt/r_0^2$.

The values of U_t were calculated according to Paterson's equation using a D_p value of 7.73×10^{-13} m^2/s. The q_t versus t curves (solid curves) derived from the U_t values are compared to experimental points and McKay curves in Fig. 5(a–e). It can be seen from the figures, the curves modeled according to Paterson's equation well fit to the experimental points whole temperature and concentration range for the constant D_p value of 7.73×10^{-13} m^2/s indicating particle-diffusion process is a dominant mechanism on the overall adsorption.

It can be concluded that from these results film-diffusion process contributes on the mechanism only at the lowest initial solution concentration because experimental data are well predicted by McKay model considered both film- and particle-diffusion. At higher concentrations, deviations between observed and calculated q_t values at especially initial fast process indicate that film-diffusion should be neglected. Furthermore, as can be deduced from the Arrhenius plot presented in the following section both D_f and D_p values calculated from the k_1 and k_2 in Fig. 4 decrease as initial concentration increases. The concentration dependence of diffusion coefficients further confirms that McKay model is not suitable to describe experimental data at higher concentrations.

3.2. Activation parameters

Both D_f values calculated from Eq. (4) by using the known surface area of the adsorbent and a film thickness of equal to mean particle radius and, D_p values computed by using Eq. (8) are temperature dependent. Thus, the energy of activation E_a and the effective diffusion coefficients D_0 for adsorption process can be determined by applying following type Arrhenius equations [38]:

$$D = D_0 \exp\left(-\frac{E_a}{RT}\right) \quad (11)$$

$$\ln D = \ln D_0 - \frac{E_a}{RT} \quad (12)$$

where T is the absolute temperature (K), R the gas constant (kJ/mol K).

The values of E_a and D_0 for film- and particle-diffusion processes are determined from $\ln D - 1/T$ plot in Fig. 6 and presented in Table 1. As it is seen from the Table 1, the effective film-diffusion coefficients corresponding to fast initial stage of adsorption process fall within a magnitude of $(0.32–1.76) \times 10^{-11}$ m^2/s whereas the effective particle-diffusion coefficients are found to be $(0.72–5.26) \times 10^{-14}$ m^2/s. On the other hand, the value of D_0 is also 7.73×10^{-13} m^2/s because D_p value calculated from Paterson's equation is independent of temperature. The reported average diffusion coefficients calculated using Bt method for 2,4-D on different

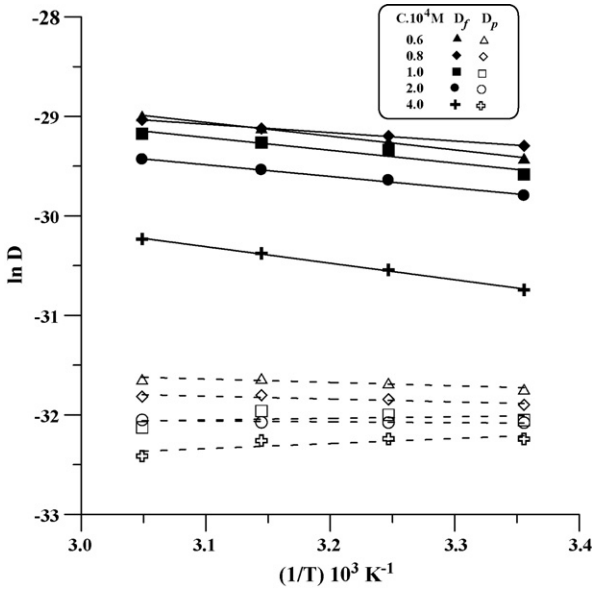

Fig. 6. Arrhenius plots drawn using film- and particle-diffusion coefficients derived according to McKay model.

activated carbon samples are in the magnitude of $\sim 10^{-12}$ m^2/s [8].

The values of E_a are positive for film-diffusion process whereas they have both negative and positive signs around zero for particle-diffusion. The E_a value for particle-diffusion according to Paterson's model is also zero. Activation energy for the particle-diffusion is that needed for the ions to jump from one lattice point to another position. Since the magnitude of E_a is related to the structure of solid particles low value is obtained for loosely packed solid particles [35,36].

Thermodynamic parameters for transition state can be determined using the following type linearized Eyring equation [38]:

$$\ln \frac{D}{T} = \ln 2.72d^2\frac{k}{h} + \frac{\Delta S^*}{R} - \frac{\Delta H^*}{T} \quad (13)$$

where k and h are Boltzmann and Planck constants, respectively and d the average distance between the successive exchanging sites, ΔS^* and ΔH^* the entropy and the enthalpy of activation, respectively. The values of ΔH^* calculated from the slope of Eyring plots (not shown here because of similarity with Arrhenius plots) are also presented in Table 1.

The values of ΔS^* were computed from the intercept using a d value of 2.6×10^{-10} m estimated using known site density and surface area of the adsorbent.

The values of Gibbs free energy of activation ΔG^* were calculated for 298 K using following well-known equation:

$$\Delta G^* = \Delta H^* - T\Delta S^* \quad (14)$$

The values of ΔS^* and ΔG^* are presented in Table 1 together with other activation parameters.

The negative ΔS^* values imply that the existence an entropy barrier in the present system and no significant change occurs in the internal structure of the BS. The values of $\Delta G^* > 0$ show that there also exists an energy barrier. The energy barrier in activated state may arise partially from hydration of 2,4-D anions in solution phase [35]. When the ions enter from the solution into the particle surface at least some of the water molecules forming hydration shell of ions are stripped off. Simultaneously, the degree of freedom of ions declines.

3.3. Effect of temperature on adsorption isotherms

The equilibrium data for 2,4-D adsorption in natural medium at different temperatures are shown in Fig. 7a. The data were fitted to the Freundlich, Dubinin–Radushkevich (D–R) and Langmuir isotherm equations.

Freundlich equation is used to describe the adsorption characteristics of the natural adsorbents because of its simplicity and excellent description of the data. The linear form of the Freundlich isotherm equation is given by [39]:

$$\ln q_e = \ln k + n \ln C_e \quad (15)$$

where k and n are the Freundlich constants. Their values are calculated from the slopes and intercepts of the straight lines of $\ln q_e$ versus $\ln C_e$ plot in Fig. 7b and presented in Table 2. The parameter k is considered as a relative measure of adsorbent

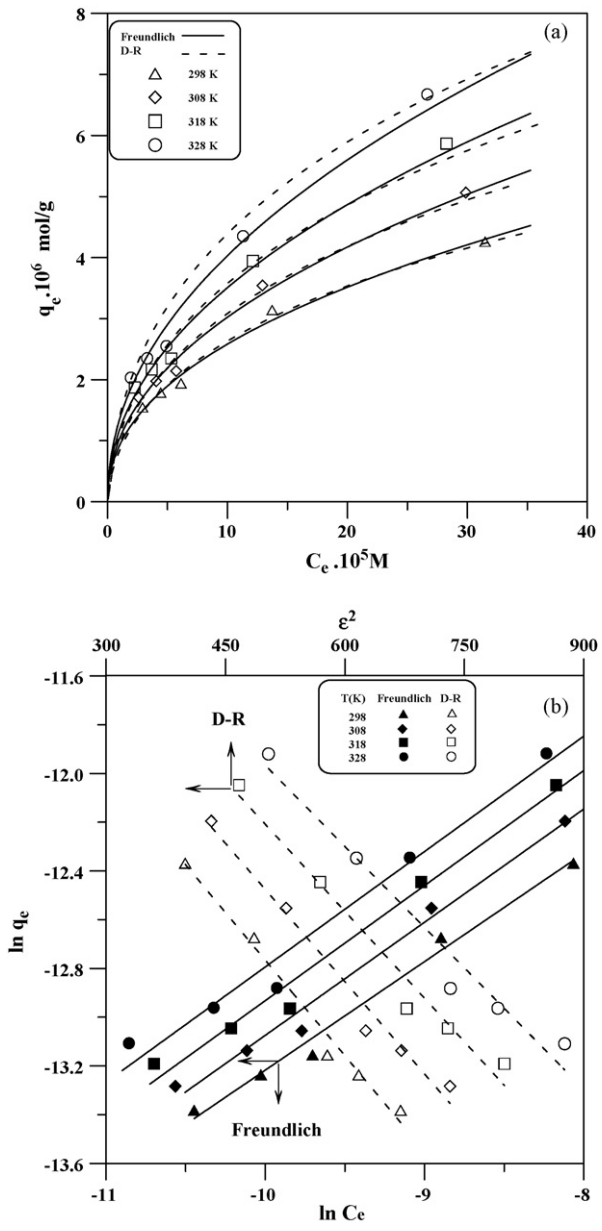

Fig. 7. (a) Adsorption isotherms of 2,4-D at different temperatures, (b) application of the data to the Freundlich and the D–R equations. (The solid and dashed curves in (a) have been calculated using the Freundlich and the D–R constants, respectively.)

Table 2
The Freundlich isotherm parameters for 2,4-D adsorption on the BS

pH	T (K)	n	$k \times 10^5$ (mol/g)	r
Natural	298	0.445	15.56	0.994
	308	0.464	21.75	0.993
	318	0.472	27.16	0.990
	328	0.473	31.59	0.987
3.5	298	0.315	3.97	0.966
4.0		0.292	3.04	0.964
5.0		0.269	2.31	0.958
5.5		0.246	1.81	0.951
6.5		0.205	1.08	0.945
7.5		0.170	0.68	0.885
8.0		0.158	0.57	0.922

capacity because the Freundlich isotherm does not into account a constant capacity. The values of the parameter n are smaller than unity, which may be correlated with surface heterogeneity. The n values close to zero are related to more heterogeneous surface [40]. The isotherm curves (solid lines) modeled according to Freundlich equation using the k and n constants presented in the Table 2 are compared in Fig. 7a to the experimental data. The equilibrium data for 2,4-D adsorption are reasonably well predicted by Freundlich isotherm equation. In the previous studies dealt with 2,4-D adsorption have also been shown that isotherm data fit well to Freundlich equation for some soil samples [6], activated carbon [8,11] and organophilic sepiolite [14].

The (D–R) isotherm parameters permit the calculation of adsorption capacity and mean adsorption energy, which defined as free energy change when one mole of ion is transferred to the surface of adsorbent from infinity in the solution.

The linearized D–R equation is given by following equation [41]:

$$\ln\ q_e = \ln\ q_m - \beta\varepsilon^2 \tag{16}$$

where q_m is the adsorption capacity of adsorbent per unit weight (mol/g), β the constant related to the mean adsorption energy (E), ε the Polanyi potential calculated from,

$$\varepsilon = RT\ ln\left(1 + \frac{1}{C_e}\right) \tag{17}$$

As shown in Fig. 7b, a plot of ln q versus ε^2, allows the estimation of q_m from the intercept and β from the slope. Mean adsorption energy is calculated from the following relation:

$$E = (-2\beta)^{-1/2} \tag{18}$$

Using the D–R constants shown in Table 3 obtained theoretical curves (dashed lines) are also in agreement with the experimental data (Fig. 7a). It has been reported that data obtained from 2,4-D adsorption on the organophilic sepiolite are well described with D–R equation [14].

Another useful model is the Langmuir isotherm equation, which assumes the monolayer coverage on an energetically identical homogeneous adsorbent surface. The linearized form of the

Table 3
The D–R isotherm parameters for 2,4-D adsorption on the BS

pH	T (K)	$q_m \times 10^6$ (mol/g)	E (kJ/mol)	r
Natural	298	20.24	11.3	0.992
	308	25.32	11.5	0.990
	318	29.71	11.8	0.986
	328	33.43	12.3	0.982
3.5	298	9.28	13.5	0.957
4.0		7.93	14.0	0.956
5.0		6.73	14.5	0.950
6.0		5.70	15.2	0.944
6.5		4.26	16.6	0.939
7.5		3.16	18.1	0.880
8.0		2.80	18.8	0.913

Table 4
The Langmuir isotherm parameters for 2,4-D adsorption on the BS

pH	T (K)	$q_m \times 10^6$ (mol/g)	K^0	ΔG^0 (kJ/mol)	r
Natural	298	5.45	10.82	−5.90	0.993
	308	7.03	8.39	−5.45	0.995
	318	7.72	10.19	−6.14	0.982
	328	8.78	10.55	−6.43	0.976
3.5	298	3.87	3.97	−6.81	0.989
4.0		3.49	3.04	−7.08	0.991
5.0		3.13	2.31	−7.39	0.994
5.5		2.81	1.81	−7.72	0.995
6.5		2.31	1.08	−8.39	0.997
7.5		1.87	0.68	−9.09	0.998
8.0		1.79	0.57	−8.83	0.998

Langmuir equation may be written as [42]:

$$\frac{C_e}{q_e} = \frac{1}{Kq_m} + \frac{1}{q_m}C_e \tag{19}$$

where K is the adsorption equilibrium constant related to the binding energy and q_m is the mono-layer capacity. The parameters of K and q_m for 2,4-D removal at different temperatures are calculated from C_e/q_e versus C_e plots (not shown here). If the equilibrium concentration C_e is expressed in molality unit, the thermodynamic adsorption equilibrium constant K^0 is found to be non-dimensional. Langmuir parameters and standard free energy changes (ΔG^0) evaluated from following equation in the temperature range from 298 to 328 are presented in Table 4:

$$\Delta G^0 = -RT\ \ln\ K^0 \tag{20}$$

The values of ΔG^0 calculated with the same way for sorption of 2,4-D on tire rubber granules have been found more negative from −12.83 to −17.26 kJ/mol when temperature increased from 285 to 230 K indicating that a more spontaneous adsorption process [8].

Standard enthalpy (ΔH^0) and entropy changes (ΔS^0) were computed as 0.81 kJ/mol and 0.02 kJ/mol K from the slope and intercept of ln K^0 versus $1/T$ plot (not shown here) drawn according to following relation:

$$\ln\ K^0 = \frac{\Delta S^0}{R} - \frac{\Delta H^0}{RT} \tag{21}$$

The low value of ΔH^0 shows that spontaneity of the reaction is entropy controlled. The values of ΔH^0 and ΔS^0 parameters for 2,4-D—tire rubber granules sorption system have been reported as 11.83 kJ/mol and 0.09 kJ/mol K, respectively [9].

It has been reported that the Langmuir model fit well to experimental data for 2,4-D adsorption on activated carbon [8,11], layered double hydroxides [15], fertilizer and steel industry wastes [10].

As it is seen from the Tables 3 and 4, the adsorption capacities calculated from the Langmuir and D–R equations increase in the order (5.45–8.78) × 10^{-6} and (2.02–3.34) × 10^{-5} mol/g as the temperature increases from 298 to 328 K, respectively. The higher capacities obtained from the D–R equation suggest that adsorbate–adsorbate interactions might be contribute on the adsorption mechanism. The more negative free energy

($E = -\Delta G^0$) values estimated from the D–R parameters may also be arising from a higher entropy change as a result of these interactions.

The reported Langmuir capacity of fertilizer industry waste (carbon slurry) is 9.60×10^{-4} mol/g. The capacities of blast furnace slag and dust of steel industry wastes have been reported as 1.36×10^{-4} and 9.50×10^{-5} mol/g whereas 2,4-D is hardly adsorbed on the sludge [10]. Adsorption capacity of 2,4-D on a chemically modified silica gel surface with the silylating agent 3-trimethoxysilylpropylamine is 4.67×10^{-5} mol/g on the other hand, capacities on zinc–aluminum–chloride layered double hydroxides increase in the range of $(1.28–5.24) \times 10^{-3}$ mol/g when Zn/Al ratios decrease from 4 to 2 [13,15]. Amounts of 2,4-D adsorbed on tire rubber granules and on organophilic sepiolite (dodecylammonium sepiolite, DAS) have been evaluated as $\sim 2.65 \times 10^{-7}$ and $\sim 4.5 \times 10^{-5}$ mol/g at initial concentrations of 1.5×10^{-5} and 4×10^{-4} M, respectively [9,14]. The adsorbents mentioned above are either specifically prepared or modified different methods except for tire rubber granules. These procedures increase the cost of adsorbents. Since the BS is a low cost high abundant material it can be considered as a suitable adsorbent for 2,4-D removal.

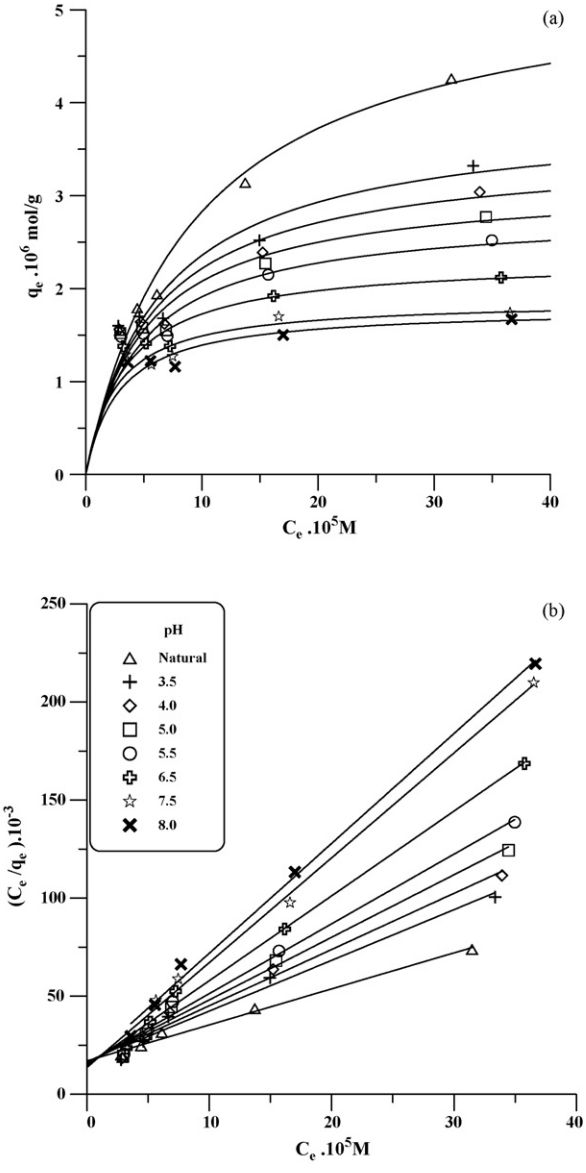

Fig. 8. (a) Adsorption isotherms of 2,4-D at different pH values (the curves have been calculated using the Langmuir constants) (b) application of the data to the Langmuir equation.

3.4. Effect of pH on adsorption isotherms

As it is seen from Fig. 8a, the equilibrium data obtained from the experiments in different initial concentrations at 298 K have been used for construction of the adsorption isotherms in the pH range from 3.5 to 8.0. It can be deduced from the Fig. 8a amount of 2,4-D adsorbed on the BS decreases with increasing pH. Since the number of protonated surface on the adsorbent increases with decreasing pH and 2,4-D ionizes to an organic anion and H^+ ion in the studied pH range ($pK_a = 2.6$). Coulombic attraction forces between more positively charged surface and 2,4-D anions are responsible for increasing adsorption with decreasing pH as reported previous studies [10,11]. Natural pH of the solutions in the studied concentration range is 5.6. Adsorption of 2,4-D on the BS remarkably decreases when ionic strength is adjusted with NaCl at the same pH region. This result suggests that Cl^- ions compete with the 2,4-D anions for the same adsorption sites on the BS surface.

Experimental data evaluated from the equilibrium conditions at different pHs were fitted to the Langmuir isotherm and depicted in Fig. 8b. Using the isotherm constants presented in the Table 4 theoretical curves were calculated and compared experimental data in Fig. 8a. As shown from the Fig. 8a, experimental data are reasonably well described by the Langmuir model. Isotherm parameters calculated according to the Freundlich and D–R equations are shown in the Tables 2 and 3, respectively.

4. Conclusions

Adsorptive removal of the herbicide 2,4-D by the BS has been studied in the concentration range of $(0.6–4.0) \times 10^{-4}$ M at different temperatures. Removal capacity of the adsorbent increased with the increasing concentration and temperature.

The kinetic data are well described with McKay model at the lowest initial concentration of 2,4-D indicating the contribution of film-diffusion on adsorption mechanisms.

Paterson's equation reasonably well fits to kinetic data points at entire concentration and temperature range studied. The constant diffusion coefficient calculated according to Paterson's equation might be useful for designing a treatment plant for removal of 2,4-D by using the BS.

Equilibrium data are quite well predicted by the Freundlich, D–R and Langmuir isotherm equations. Freundlich exponents lower than unity indicate favorable adsorption. Thermodynamic parameters for activated state, $\Delta E^* > 0$, $\Delta H^* > 0$, $\Delta G^* > 0$ and $\Delta S^* < 0$, show that both energy and entropy barrier exist in the system. Although an energy barrier is available in the transition state free energy change ($\Delta G^0 < 0$) evaluated using

thermodynamic adsorption equilibrium constant derived from the Langmiur equation indicate that adsorption of 2,4-D on the BS is a spontaneous process.

The increase of adsorption capacity with decreasing pH shows that 2,4-D anions are preferred on positively charged adsorption sites while it decreases because of a competition between 2,4-D anions and Cl^- ions arising from inert electrolyte used for the ionic strength adjustment.

References

[1] G. Haberhauer, L. Pfeiffer, M.H. Gerzabek, Influence of molecular structure on sorption of phenoxyalkanoic herbicides on soil and its particle size fractions, J. Agric. Food Chem. 48 (2000) 3722–3727.

[2] G. Akçay, M. Akçay, K. Yurdakoç, The characterization of prepared organo-montmorillonite (DEDMAM) and sorption of phenoxyalkanoic acid herbicides from aqueous solution, J. Colloid Interface Sci. 296 (2006) 428–433.

[3] J. Inacio, C. Taviot-Gueho, C. Forano, J.P. Besse, Adsorption of MCPA pesticide by MgAl-layered double hydroxides, Appl. Clay Sci. 18 (2001) 255–264.

[4] L.P. Cardoso, J.B. Valim, Study of acids herbicides removal by calcined Mg–Al–CO_3–LDH, J. Phys. Chem. Solids 67 (2006) 987–993.

[5] E. Tütem, R. Apak, Ç.F. Ünal, Adsorptive removal of chlorophenols from water by bituminous shale, Wat. Res. 8 (1998) 2315–2324.

[6] M. Al Kuisi, Adsorption of dimethoate and 2,4-D on Jordan Valley soils and their environmental impacts, Environ. Geol. 42 (2002) 666–671.

[7] I.G. Dubus, E. Bariusso, R. Calvet, Sorption of weak organic acids in soils: clofencet, 2,4-D and salicylic acid, Chemosphere 45 (2001) 767–774.

[8] P. Chingombe, B. Saha, R.J. Wakeman, Effect of surface modification of an engineered activated carbon on the sorption of 2,4-dichlorophenoxy acetic acid and benazolin from water, J. Colloid Interface Sci. 297 (2006) 434–442.

[9] J.B. Alam, A.K. Dikshit, M. Bandyopadhayay, Evaluation of thermodynamic properties of sorption of 2,4-D and atrazine by tire rubber granules, Sep. Purif. Technol. 42 (2005) 85–90.

[10] V.K. Gupta, I. Ali, Suhas, V.K. Saini, Adsorption of 2,4-D and carbofuran pesticides using fertilizer and steel industry wastes, J. Colloid Interface Sci. 299 (2006) 556–563.

[11] Z. Aksu, E. Kabasakal, Batch adsorption of 2,4-dichlorophenoxy-acetic acid (2,4-D) from aqueous solution by granular activated carbon, Sep. Purif. Technol. 35 (2004) 223–240.

[12] A.G.S. Prado, C. Airoldi, Adsorption, preconcentration the herbicide 2,4-dichlorophenoxyacetic acid, Fresenius J. Anal. Chem. 371 (2001) 1028–1030.

[13] A.G.S. Prado, C. Airoldi, Adsorption, preconcentration and separation of cations on silica gel chemically modified with the herbicide 2,4-dichlorophenoxyacetic acid, Anal. Chim. Acta 432 (2001) 201–211.

[14] G. Akçay, M. Akçay, Kadir Yurdakoç, Removal of 2,4-dichlorophenoxyacetic acid from aqueous solutions by partially characterized organophilic sepiolite: thermodynamic and kinetic calculations, J. Colloid Interface Sci. 281 (2005) 27–32.

[15] A. Legrouria, M. Lakraimib, A. Barrougb, A. De Royc, J.P. Bessec, Removal of the herbicide 2,4-dichlorophenoxyacetate from water to zinc–aluminium–chloride layered double hydroxides, Wat. Res. 39 (2005) 3441–3448.

[16] Z. Al-Qodaha, A.T. Shawaqfeh, W.K. Lafi, Adsorption of pesticides from aqueous solutions using oil shale ash, Desalination 208 (2007) 294–305.

[17] A. Parker, J.E. Rate, Environmental Interactions of Clays and the Environment, Springer-Verlag, Berlin, Germany, 1998.

[18] P. Benoit, E. Barriuso, R. Calvet, Biosorption characterization of herbicides, 2,4-D and Atrazine, and two chlorophenols on fungal mycelium, Chemosphere 37 (1998), 1271-128.

[19] J.J. Pignatello, B. Xing, Mechanism of slow sorption of organic chemicals to natural particles, Environ. Sci. Technol. 30 (1995) 1–11.

[20] P.M. Jones, Bituminous Materials, National Research Council Canada, Canadian Building Digests, CBD 38, 1963, 01–02.

[21] S. Aliyev, B. Koralay, N. Sonel, S. Koç, S. Imer, Organic carbon and trace metal distribution in the Gökçesu shale: Eocene Basin, Bolu-Turkey, Energy Sour., Part A 29 (2007) 591–605.

[22] L. Ballice, J.W. Larsen, Changes in the cross-link density of Goynuk oil shale (Turkey) on pyrolysis, Fuel 82 (2003) 1305–1310.

[23] E. Putun, A. Akar, E. Ekinci, K.D. Bartle, Chemistry and geochemistry of Turkish oil shale kerogens, 67, 1988, 1106–1110.

[24] M. Önal, T. Ayyıldız, Y. Önal, C. Akmil-Başar, Stratigraphic, mineralogic and geochemical characterization of Gürün oil shales, central Anatolia, Turkey, Oil Shale 23 (4) (2006) 297–312.

[25] W.D. Smith, N.D. Naylor, Oil shale resources of Nova Scotia. Department of Mines and Energy, Econ. Jeol. Series 3 (1990) 274–354.

[26] N.E. Altun, Cahit Hicyilmaz, J.Y. Hwang, A.S. Bağcı, Evaluation of a Turkish low quality oil shale by flotation as a clean energy source: material characterization and determination of flotation behavior, Fuel Process. Technol. 87 (2006) 783–791.

[27] A.Y. Al-Otoom, Utilization of oil shale in the production of Portland clinker, Cem. Concr. Compos. 28 (2006) 3–11.

[28] M.L.G. Hourcade, C. Torrente, M.A. Galan, Study of the solubility of kerogen from oil shales (Puertollano, Spain) in supercritical toluene and methanol, Fuel 86 (2007) 698–705.

[29] B.Z. Uysal, A. Tamimi, Parametric investigation of oil shale extraction with organic solvents, Sep. Sci. Technol. 25 (1990) 1151–1155.

[30] R.A. Shawabkeh, Adsorption of chromium ions from aqueous solution by using activated carbo-aluminosilicate material from oil shale, J. Colloid Interface Sci. 299 (2006) 530–536.

[31] A.N.A. El-Hendawy, Surface and adsorptive properties of carbons prepared from biomass, Appl. Surf. Sci. 252 (2005) 287–295.

[32] A.N.A. El-Hendawy, Variation in the FTIR spectra of a biomass under impregnation, carbonization and oxidation conditions, J. Anal. Appl. Pyrol. 75 (2006) 159–166.

[33] H. MacKay, Kinetics of isotopic exchange reactions, Nature 142 (1938) 997–998.

[34] F. Helferich, Ion Exchange, McGraw-Hill, NY, 1962.

[35] T.C. Huang, F.N. Tsai, Kinetic studies on the isotopic exchange of calcium ion and calcium carbonate, J. Inorg. Nucl. Chem. 32 (1970) 17–31.

[36] T.C. Huang, K.Y. Li, S.C. Hoo, Mechanism of isotopic exchange reaction between calcium ion and calcium oxalate, J. Inorg. Nucl. Chem. 34 (1972) 47–55.

[37] A.E. Kurtoğlu, G. Atun, Determination of kinetics and equilibrium of Pb/Na exchange on clinoptilolite, Sep. Purif. Technol. 50 (2006) 62.

[38] A.C. Wahl, N.A. Bonner, Radioactivity Applied to Chemistry, John Wiley and Sons, Inc., New York, 1958.

[39] H. Freundlich, Über die Adsorption in Lösungen, Z. Physik. Chem. 57 (1907) 385–470.

[40] G. Sposito, The Thermodynamics of Soil Solutions, 1st ed., Clarendon, Oxford, 1981.

[41] M.M. Dubinin, L.V. Radushkevich, Equation of the characteristic curve of activated charcoal, Chem. Zentr. 1 (1947) 875–889.

[42] I. Langmuir, The adsorption of gases on plane surfaces of glass, mica and platinum, J. Am. Chem. Soc. 40 (1918) 1361–1403.